

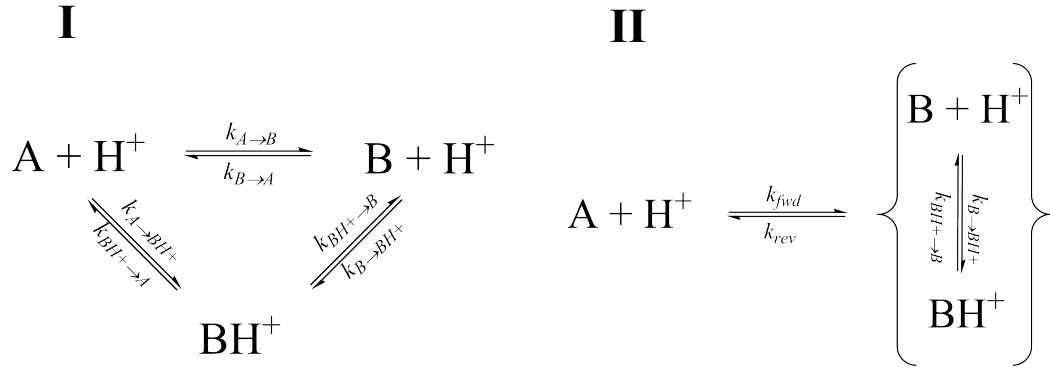
Supporting information for:

The complexity of protein energy landscapes studied by solution NMR relaxation dispersion experiments

Gennady Khirich¹ and J. Patrick Loria^{1,2}*

¹Department of Chemistry, 225 Prospect Street, New Haven, CT 06520, ²Department of Molecular Biophysics and Biochemistry, 260 Whitney Avenue, New Haven, CT 06520

A6.1. k_{ex} vs. pH for Scheme 1 (Dynamic Cluster 1)



$$\frac{1}{k_{ex}} = \frac{1}{k_{A \rightarrow B}} + \frac{1}{k_{B \rightarrow A}} + \frac{1}{k_{BH^+ \rightarrow B}} + \frac{1}{k_{B \rightarrow BH^+}[H^+]} + \frac{1}{k_{BH^+ \rightarrow A}} + \frac{1}{k_{A \rightarrow BH^+}[H^+]} \quad \text{SI-1.1}$$

$$k_{ex} = \left[\frac{1}{k_{A \rightarrow B}} + \frac{1}{k_{B \rightarrow A}} + \frac{1}{k_{BH^+ \rightarrow B}} + \frac{1}{k_{BH^+ \rightarrow A}} + \frac{1}{[H^+]} \left(\frac{1}{k_{B \rightarrow BH^+}} + \frac{1}{k_{A \rightarrow BH^+}} \right) \right]^{-1} \quad \text{SI-1.2}$$

Let

$$\frac{1}{k_{ex}^{(conf)}} \equiv \frac{1}{k_{A \rightarrow B}} + \frac{1}{k_{B \rightarrow A}} + \frac{1}{k_{BH^+ \rightarrow B}} + \frac{1}{k_{BH^+ \rightarrow A}} \approx \frac{1}{k_{A \rightarrow B}} + \frac{1}{k_{B \rightarrow A}} + \frac{1}{k_{BH^+ \rightarrow A}} \quad \text{SI-1.3}$$

and

$$\frac{1}{k_{ex}^{(prot)}} \equiv \frac{1}{k_{B \rightarrow BH^+}} + \frac{1}{k_{A \rightarrow BH^+}}, \quad \text{SI-1.4}$$

with the approximation that $k_{BH^+ \rightarrow B}$ is multiple orders of magnitude larger than the other rate constants appearing in equation SI-1.3. Thus, by inserting eqs SI-1.3 and SI-1.4 into equation SI-1.2, combined with the fact that $pH = -\log[H^+]$, we get the final expression for k_{ex} as a function of pH for dynamic cluster 1:

$$k_{ex}(pH) = \left[\frac{1}{k_{ex}^{(conf)}} + \frac{10^{pH}}{k_{ex}^{(prot)}} \right]^{-1} \quad \text{SI-1.5}$$

Temperature	$k_{ex} \pm \delta k_{ex}$ (s ⁻¹)	$k_{ex} \pm \delta k_{ex}$ (s ⁻¹)	$k_{ex} \pm \delta k_{ex}$ (s ⁻¹)	$k_{ex} \pm \delta k_{ex}$ (s ⁻¹)
	pH 7.0	pH 6.4	pH 5.5	pH 4.5
Dynamic Cluster 1				
25°C	1,971 ± 51	2,652 ± 99	N.Q.	13,384 ± 1,177*
20°C	1,497 ± 41	1,901 ± 57	> 4,000	N.D.
15°C	1,190 ± 35	1,469 ± 52	~3,200	N.A.
10°C	977 ± 37	1,103 ± 40	2,039 ± 170	N.D.
Dynamic Cluster 2				
25°C	1,599 ± 74	1,758 ± 96	1,469 ± 52	2,081 ± 337
20°C	966 ± 49	1,154 ± 48	1,103 ± 40	1,883 ± 310
15°C	725 ± 40	780 ± 53	847 ± 75	N.A.
10°C	478 ± 49	465 ± 29	581 ± 49	1,231 ± 287

SI Table 1: Globally-derived k_{ex} values with their uncertainties for both dynamic clusters in RNase A in the temperature range 10 – 25°C and the pH range 4.5 – 7.0. All k_{ex} values were obtained from CPMG relaxation dispersion experiments. N.D. means no dispersion was detected at these conditions; N.Q. means dispersion is present but outside the limits of quantitation with CPMG methodology; N.A. means not applicable since data at these conditions were not collected. The following residues were included in global analyses of CPMG data: S16, T17, F46, V47, A64, K66, T70, N71, T82, D83, and Q101 at pH 7.0; S15, S16, T17, F46, A64, K66, T70, N71, T82, D83, and Q101 at pH 6.4; F46, A64, K66, T70, N71, D83 and T100 at pH 5.5; and K66 and N71 at pH 4.5. Global analysis of off-resonance $R_{Iq} - R_I$ dispersion data at pH 4.5 and 25°C involved S15, F46, V47, H48, A64, K66, T70, N71, T82, D83, and T100.

Temperature	$k_{fwd} \pm \delta k_{fwd} \text{ (s}^{-1}\text{)}$	$k_{fwd} \pm \delta k_{fwd} \text{ (s}^{-1}\text{)}$	$k_{fwd} \pm \delta k_{fwd} \text{ (s}^{-1}\text{)}$	$k_{fwd} \pm \delta k_{fwd} \text{ (s}^{-1}\text{)}$
	pH 7.0	pH 6.4	pH 5.5	pH 4.5

Dynamic Cluster 1

25°C	124 ± 8	225 ± 20	N.Q.	N.Q.
20°C	83 ± 5	138 ± 10	N.Q.	N.Q.
15°C	76 ± 4	106 ± 7	N.Q.	N.Q.
10°C	65 ± 4	76 ± 4	N.Q.	N.Q.

Dynamic Cluster 2

25°C	65 ± 15	72 ± 16	81 ± 18	85 ± 23
20°C	35 ± 6	41 ± 7	46 ± 8	67 ± 15
15°C	21 ± 4	22 ± 4	24 ± 5	N.A.
10°C	12 ± 3	11 ± 2	14 ± 3	30 ± 9

SI Table 2: Globally-derived k_{fwd} values with their uncertainties for both dynamic clusters in RNase A in the temperature range 10 – 25°C and the pH range 4.5 – 7.0. All k_{fwd} values were obtained from globally-derived values of k_{ex} and p_B from CPMG relaxation dispersion experiments. N.Q. means not quantifiable as the system is in fast exchange under these conditions and the measurement of kinetic and thermodynamic exchange parameters was not possible; N.A. means not applicable since data at these conditions were not collected.

Temperature	$k_{rev} \pm \delta k_{rev} (s^{-1})$	$k_{rev} \pm \delta k_{rev} (s^{-1})$	$k_{rev} \pm \delta k_{rev} (s^{-1})$	$k_{rev} \pm \delta k_{rev} (s^{-1})$
	pH 7.0	pH 6.4	pH 5.5	pH 4.5
Dynamic Cluster 1				
25°C	1,847 ± 48	2,427 ± 93	N.Q.	N.Q.
20°C	1,415 ± 39	1,762 ± 54	N.Q.	N.A.
15°C	1,113 ± 33	1,363 ± 48	N.Q.	N.A.
10°C	912 ± 35	1,027 ± 37	N.Q.	N.A.
Dynamic Cluster 2				
25°C	1,534 ± 72	1,670 ± 91	1,901 ± 100	2,021 ± 329
20°C	932 ± 47	1,105 ± 46	1,234 ± 90	1,821 ± 301
15°C	704 ± 39	756 ± 51	827 ± 74	N.A.
10°C	467 ± 48	451 ± 28	570 ± 48	1,206 ± 282

SI Table 3: Globally-derived k_{rev} values with their uncertainties for both dynamic clusters in RNase A in the temperature range 10 – 25°C and the pH range 4.5 – 7.0. k_{rev} values were either obtained from globally-derived values of k_{ex} and p_A from CPMG relaxation dispersion experiments, or estimated using $k_{rev} \approx k_{ex}$ when the system was in sufficiently fast exchange. N.Q. means not quantifiable as the system is in fast exchange under these conditions and the measurement of kinetic and thermodynamic exchange parameters was not possible; N.A. means not applicable since data at these conditions were not collected.

Temperature	$P_A \pm \delta P_A$	$P_A \pm \delta P_A$	$P_A \pm \delta P_A$	$P_A \pm \delta P_A$
	pH 7.0	pH 6.4	pH 5.5	pH 4.5
Dynamic Cluster 1				
25°C	0.937 ± 0.004	0.915 ± 0.007	N.Q.	N.Q.
20°C	0.945 ± 0.003	0.927 ± 0.005	N.Q.	N.Q.
15°C	0.936 ± 0.003	0.928 ± 0.004	N.Q.	N.Q.
10°C	0.934 ± 0.003	0.931 ± 0.003	N.Q.	N.Q.
Dynamic Cluster 2				
25°C	0.956 ± 0.003	0.950 ± 0.004	0.960 ± 0.004	0.971 ± 0.014
20°C	0.965 ± 0.001	0.956 ± 0.002	0.969 ± 0.003	0.967 ± 0.016
15°C	0.970 ± 0.001	0.968 ± 0.001	0.977 ± 0.001	N.A.
10°C	0.975 ± 0.001	0.970 ± 0.001	0.980 ± 0.010	0.980 ± 0.008

SI Table 4: Globally-derived p_A values with their uncertainties for both dynamic clusters in RNase A in the temperature range 10 – 25°C and the pH range 4.5 – 7.0 from CPMG relaxation dispersion experiments. N.Q. means not quantifiable as the system is in fast exchange under these conditions and the measurement of kinetic and thermodynamic exchange parameters was not possible; N.A. means not applicable since data at these conditions were not collected.

Energetic	pH 7.0	pH 6.4	pH 5.5	pH 4.5
Quantity	(kcal mol⁻¹)	(kcal mol⁻¹)	(kcal mol⁻¹)	(kcal mol⁻¹)
E_a	7.80 ± 0.52	9.67 ± 0.44	N.Q.	N.Q.
E_{a,fwd}	7.88 ± 0.46	11.81 ± 0.88	N.Q.	N.Q.
E_{a,rev}	7.88 ± 0.46	9.50 ± 0.38	N.Q.	N.Q.
ΔH	0	2.31 ± 0.80	N.Q.	N.Q.
ΔH[†]_{fwd}	7.30 ± 0.46	11.24 ± 0.88	N.Q.	N.Q.
ΔH[†]_{rev}	7.30 ± 0.46	8.92 ± 0.38	~17	N.Q.
TΔS	-1.61 ± 0.03	0.88 ± 0.82	N.Q.	N.Q.
TΔS[†]_{fwd}	-7.30 ± 0.46	-3.03 ± 0.90	N.Q.	N.Q.
TΔS[†]_{rev}	-5.69 ± 0.47	-3.91 ± 0.38	~5	N.Q.
ΔG	1.57 ± 0.02	1.45 ± 0.02	N.Q.	N.Q.
ΔG[†]_{fwd}	14.42 ± 0.33	14.19 ± 0.27	N.Q.	N.Q.
ΔG[†]_{rev}	12.85 ± 0.33	12.73 ± 0.27	~12.38 ± 0.30	~11.87 ± 0.42

SI Table 5: Global activation and thermodynamic parameters, along with their uncertainties, for dynamic cluster 1 in the pH range 4.5 – 7.0. All values are in kcal/mol. Entropy terms are reported at 25°C. Values that are labeled N.Q. could not be quantified or estimated due to the system being in fast exchange. All Gibbs free energies are reported as average values between 10 and 25°C.

Energetic	pH 7.0	pH 6.4	pH 5.5	pH 4.5
Quantity	(kcal mol⁻¹)	(kcal mol⁻¹)	(kcal mol⁻¹)	(kcal mol⁻¹)
E_a	13.07 ± 1.02	14.67 ± 0.47	13.67 ± 0.52	6.03 ± 0.84
$E_{a,\text{fwd}}$	19.17 ± 0.66	20.77 ± 0.42	19.77 ± 0.59	12.04 ± 1.32
$E_{a,\text{rev}}$	12.88 ± 1.03	14.47 ± 0.48	13.47 ± 0.51	5.84 ± 0.84
ΔH	6.30 ± 0.43	6.30 ± 0.43	6.30 ± 0.43	6.30 ± 0.43
$\Delta H_{\text{fwd}}^\ddagger$	18.60 ± 0.70	20.20 ± 0.42	19.20 ± 0.84	11.46 ± 1.32
$\Delta H_{\text{rev}}^\ddagger$	12.30 ± 1.03	13.86 ± 0.50	12.90 ± 0.51	5.26 ± 0.84
$T\Delta S$	4.44 ± 0.44	4.44 ± 0.44	4.44 ± 0.44	4.44 ± 0.44
$T\Delta S_{\text{fwd}}^\ddagger$	3.62 ± 0.68	5.30 ± 0.43	4.36 ± 0.60	-3.22 ± 0.97
$T\Delta S_{\text{rev}}^\ddagger$	-0.82 ± 1.05	0.83 ± 0.51	-0.08 ± 0.52	-25.68 ± 2.89
ΔG	1.97 ± 0.05	1.97 ± 0.05	1.97 ± 0.05	1.97 ± 0.05
$\Delta G_{\text{fwd}}^\ddagger$	15.07 ± 0.73	15.03 ± 0.36	14.95 ± 0.37	14.20 ± 0.60
$\Delta G_{\text{rev}}^\ddagger$	13.10 ± 0.73	13.05 ± 0.37	12.98 ± 0.36	12.73 ± 0.59

SI Table 6: Global activation and thermodynamic parameters, along with their uncertainties, for dynamic cluster 2 in the pH range 4.5 – 7.0. All energies are in kcal/mol. Entropy terms are reported at 25°C. All Gibbs free energies are reported as average values between 10 and 25°C.

Residue	pH 7.0	pH 6.4	pH 5.5	pH 4.5
	$\Delta\omega \pm \delta\Delta\omega$ (ppm)	$\Delta\omega \pm \delta\Delta\omega$ (ppm)	$\Delta\omega \pm \delta\Delta\omega$ (ppm)	$\Delta\omega \pm \delta\Delta\omega$ (ppm)
S15	N.D.	0.94 ± 0.03	N.Q.	N.D.
S16	-0.99 ± 0.02	-1.28 ± 0.03	O.L.	N.D.
T17	2.40 ± 0.07	3.45 ± 0.12	N.P.	N.P.
F46	1.20 ± 0.03	1.68 ± 0.05	N.Q.	N.D.
V47	2.13 ± 0.06	N.D.	N.Q.	N.D.
T82	3.25 ± 0.11	3.72 ± 0.14	O.L.	N.D.
D83	1.74 ± 0.04	2.35 ± 0.07	N.Q.	N.D.
Q101	-2.44 ± 0.07	-3.31 ± 0.11	O.L.	O.L.
A64	0.86 ± 0.02	0.87 ± 0.02	0.85 ± 0.03	N.D.
K66	$+3.18 \pm 0.11$	$+2.97 \pm 0.11$	$+3.09 \pm 0.15$	$+2.86 \pm 0.73$
T70	-0.95 ± 0.03	-0.94 ± 0.02	-1.06 ± 0.04	N.D.
N71	2.64 ± 0.07	2.53 ± 0.07	2.40 ± 0.10	$2.31 \pm 0.53^*$

SI Table 7: $\Delta\omega$ for residues in dynamic clusters 1 and 2, as measured by global fitting of CPMG relaxation dispersion data. Explicit signs of $\Delta\omega$ are given where previous experimental data is available¹⁶. N.Q. means dispersion is present but outside the limits of quantitation with CPMG methodology; N.D. indicates lack of detectable CPMG dispersion at least at one static field strength and temperature at a given pH; O.L. signifies an overlapped peak; and N.P. indicates a peak that extends below the baseline.

T (°C)	$k_{ex}^{(conf)}$ (s⁻¹)	error (s⁻¹)	$k_{ex}^{(prot)}$ (s⁻¹)	error (s⁻¹)
25	13,976	1,279	9.74E+09	4.41E+09
20	4,312	944.5	1.25E+10	7.48E+09
15	3,477	809.1	9.41E+09	5.89E+09
10	2,024	471.7	1.14E+10	8.55E+09
$E_a^{(conf)}$ (kcal/mol)				
22.8 +/- 4.0			$E_a^{(prot)}$ (kcal/mol)	
			~ 0	

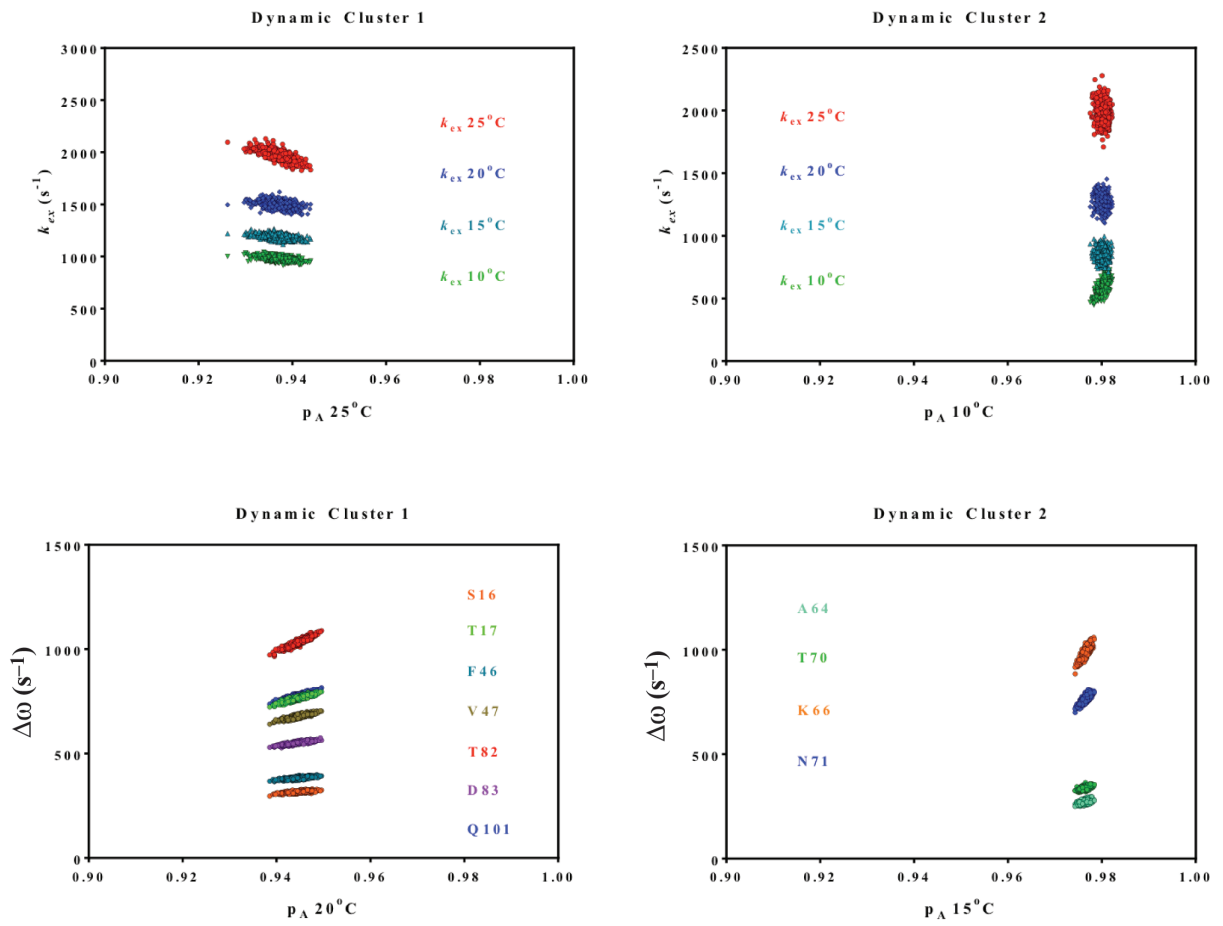
SI Table 8: Temperature Dependence of $k_{ex}^{(conf)}$ and $k_{ex}^{(prot)}$ and their associated apparent activation barriers.

Condition	$\Delta\omega$ (ppm)	$\Delta\omega$ error (ppm)	k_{ex} (s^{-1})	k_{ex} error (s^{-1})	p_A	p_A error
WT	5.40	0.30	1,215	240	0.9951	0.0003
Loop1 _{ECP}	3.84	1.30	651	1,440	0.9975	0.0034
H48A [*]	5.42		1,215		0.9957	
D121A	5.42	0.36	1,522	331	0.9957	0.0003
D121N [*]	5.42		1,215		0.9936	
D121A/N [‡]	5.57	0.27	1,466	255	0.9957	0.0002
T82A	N.D.		N.D.		N.D.	
T17A	4.65	0.33	539	424	0.9936	0.0039
Buffers [#]	5.22	0.41	1,210	384	0.9959	0.0004

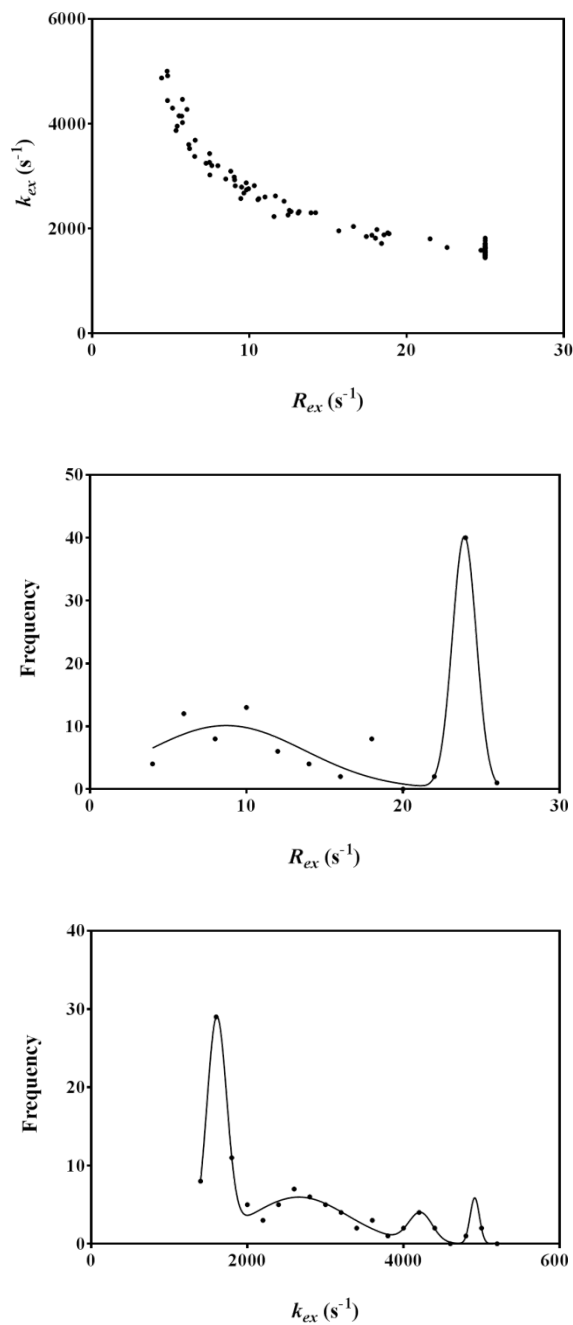
SI Table 9: ^{*}Dispersion data was reasonably fit using WT dynamics parameters due to noise (H48A) or only having single field data (D121N). [‡]D121A and D121N dispersion data were fit simultaneously; this was not a double mutant. [#]Dispersion data under various buffer conditions, such as SO_4^{-2} , PO_4^{-3} , CH_3COO^- , at pH 7.0 and 25°C, were fit simultaneously as only single-field data was available. N.D. signifies no discernible dispersion.

Energetic Quantity	Measured Value for R33 (kcal mol⁻¹)
$E_{a,\text{fwd}}$	21.0
$E_{a,\text{rev}}$	≤ 21.0
ΔH	0
$\Delta H_{\text{fwd}}^{\ddagger}$	≤ 20.5
$\Delta H_{\text{rev}}^{\ddagger}$	≤ 20.5
$T\Delta S$	-3.2 ± 0.04
$T\Delta S_{\text{fwd}}^{\ddagger}$	≤ 4.1
$T\Delta S_{\text{rev}}^{\ddagger}$	≤ 7.2
ΔG	3.2 ± 0.04
$\Delta G_{\text{fwd}}^{\ddagger}$	≤ 16.5
$\Delta G_{\text{rev}}^{\ddagger}$	≤ 13.4

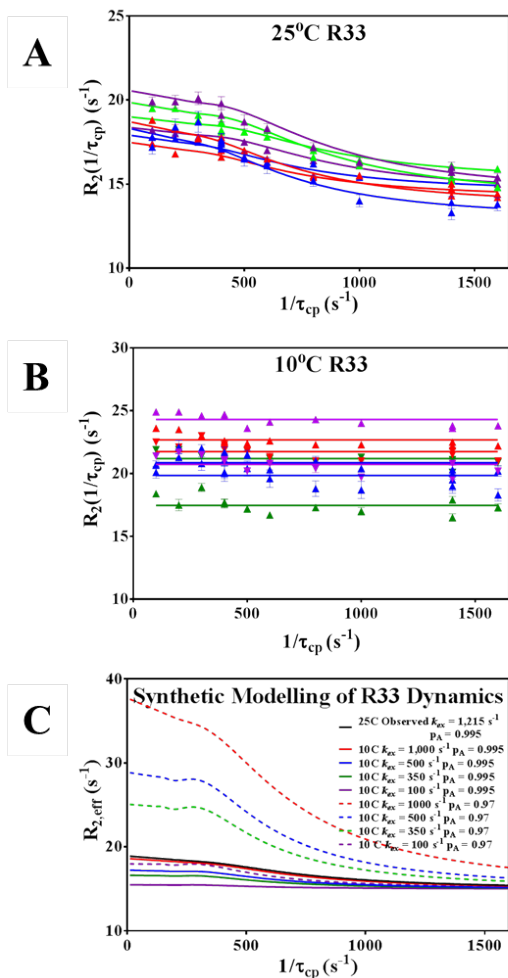
SI Table 10. Thermodynamic quantities for Arg33. Values of the activation parameters represent lower boundaries and thus the uncertainties are not included. The uncertainty for ΔH is not listed as the temperature dependence of the populations was fit with a horizontal line (slope = 0). The values of these parameters were found to remain unchanged in the pH range 4.5 – 7.0.



SI Figure 1: Monte Carlo simulations.

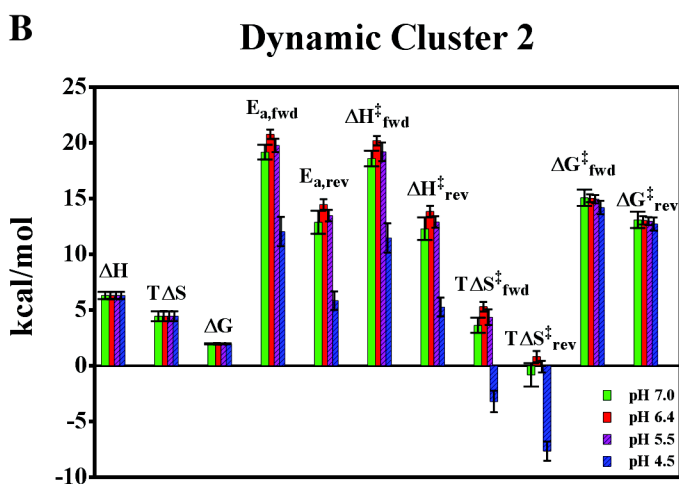
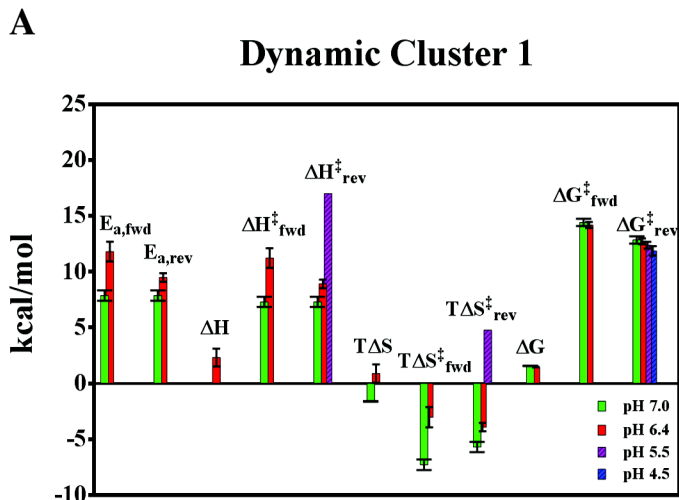


SI Figure 2: $R_{I\rho}$ Monte Carlo simulation results of dynamic cluster 2 at 25°C and pH 4.5 using CPMG-obtained dynamic parameters ($k_{ex} = 2,100 \text{ s}^{-1}$, $R_{ex} = 15 \text{ s}^{-1}$) as input for eqs 1.11 and 1.13. Clear correlations between k_{ex} and R_{ex} are seen, which result in the overestimation of k_{ex} by a factor of two when the experimental dispersion data is fit with these equations.

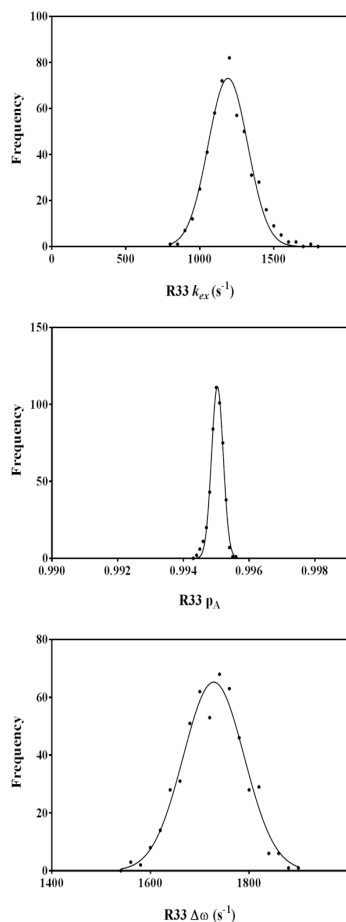


SI-Figure 3: The CPMG dispersion profiles of R33 at (A) 25°C and (B) 10°C at 500 (▼) and 600 (▲) MHz at pH 7.0 (green), 6.4 (red), 5.5 (purple), and 4.5 (blue). At 25°C, $k_{ex} = 1,215 \pm 240 \text{ s}^{-1}$, $p_a = 99.5 \pm 0.03\%$, and $\Delta\omega = 5.41 \pm 0.30 \text{ ppm}$. At 10°C, the dispersion profiles were best modeled by horizontal lines ($R_{ex} < 1.5 \text{ s}^{-1}$). (C) Monte Carlo validation of noise-corrupted best-fit CPMG parameters from R33 relaxation dispersion analysis at 25°C in the pH range 4.5 – 7.0. (D) A synthetic justification for the observed temperature dependence of the relaxation dispersion profiles of R33 between pH 4.5 and 7.0. The legend and color scheme are provided as an inset. An initial dispersion profile based on the measured global parameters at 25°C (with R_2^0

= 15 s⁻¹) was generated. Further relaxation profiles were generated by gradually decreasing k_{ex} to 100 s⁻¹, with p_A either remaining constant at the observed 25°C value of 99.5%, or decreasing modestly to 97%, for each value of k_{ex} . $\Delta\omega$, was assumed to be temperature-independent. All cases corresponding to the decrease in p_A resulted in a clear elevation in the amplitude of the dispersion curves relative to the initial 25°C profile for all decreasing values of k_{ex} , which is not what is experimentally observed. However, when p_A was held constant at 99.5%, each consecutively lower value of k_{ex} led to a reduction in the amplitude of the dispersion profile, in agreement with the observations at 10°C at each pH. Thus, it appears that the populations of R33 are insensitive to changes in temperature and remain highly skewed in the pH range 4.5 – 7.0. An upper boundary to k_{ex} at 10°C may be estimated as being 350 s⁻¹, as lower values of k_{ex} result in the amplitude of the synthetic profiles becoming less than 1.5 s⁻¹, in agreement with what is observed. The thermodynamic parameters and the upper boundaries to the activation parameters of R33 are given in SI Table 10.

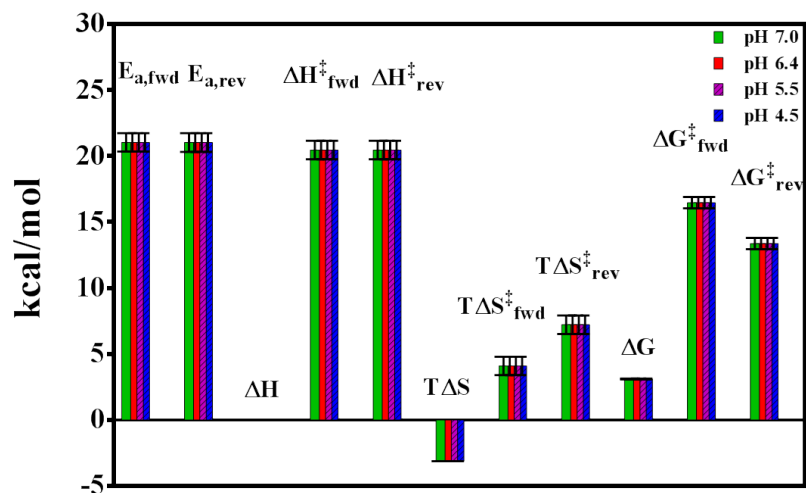


SI-Figure 4. Summary of the pH dependence of activation parameters and thermodynamics of conformational motions in clusters 1 and 2. All entropic terms were calculated at 25° C, and all Gibbs free energies are the average values across the temperature range 10 – 25° C. All data was measured directly from CPMG dispersion, except the parameters reported for cluster 1 at pH 5.5, and 4.5, which were estimated assuming skewed global populations ($k_{ex} \approx k_{rev}$).

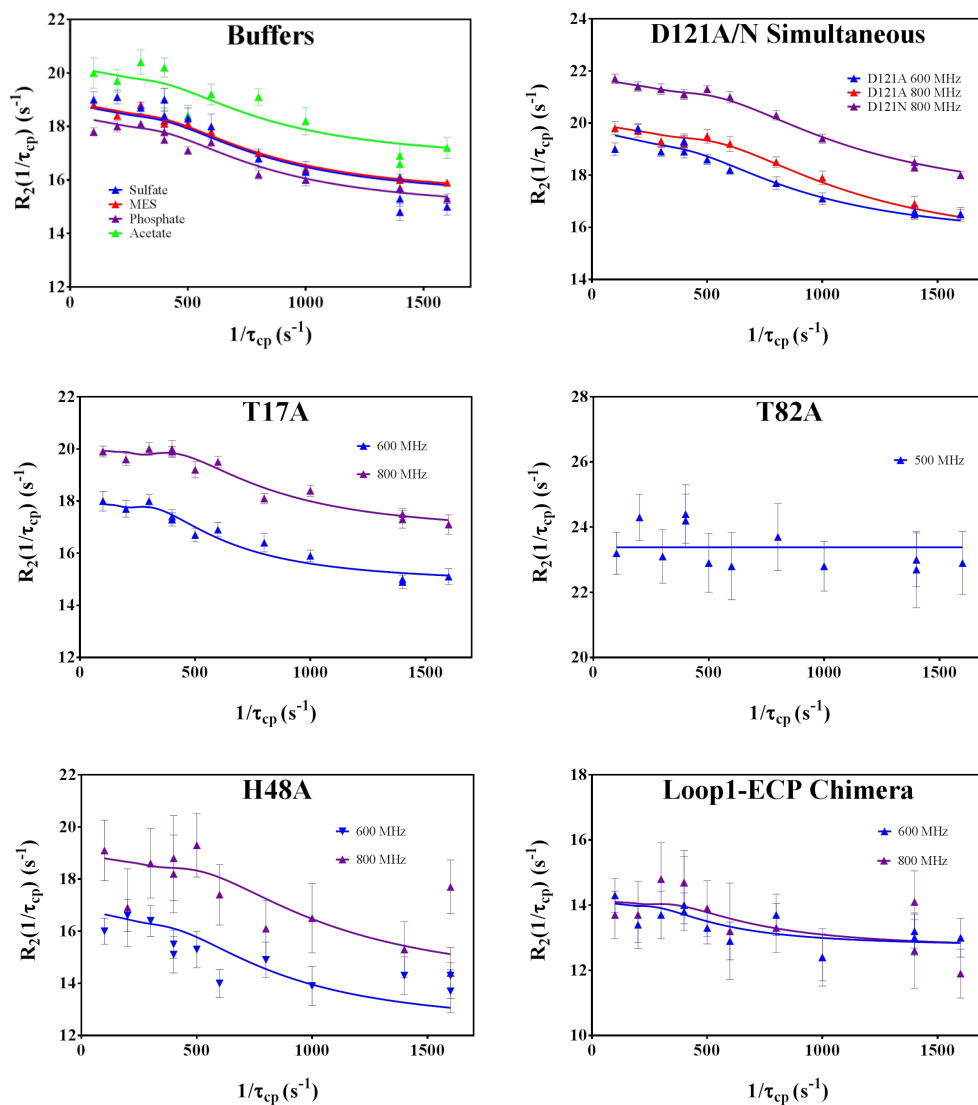


SI Figure 5 Monte Carlo simulation of the backbone dynamics of R33 at 25°C in the pH range 4.5 – 7.0. The two-field data at these conditions were best modeled by values of p_A and $\Delta\omega$ (simulated at 500MHz) that do not vary with pH. The input parameters of $k_{ex} = 1,215 s^{-1}$, $p_A = 99.5\%$, and $\Delta\omega = 1,722 s^{-1}$ have been accurately reproduced from the noise-corrupted synthetic data sets.

R33



SI-Figure 5: Estimates of the activation and thermodynamic parameters of the backbone amide motion of residue R33. These values were found to not be affected by pH, or the presence of small buffer solute molecules such as acetate, phosphate, or sulfate. The values of $E_{a,fwd/rev}$, $\Delta H^{\ddagger}_{fwd/rev}$, $T\Delta S^{\ddagger}_{fwd/rev}$ (at 25°C), and $\Delta G^{\ddagger}_{fwd/rev}$ depicted here represent estimates of their lower boundaries.



SI-Figure 6: CPMG relaxation dispersion analysis of R33 under various buffer and mutagenic conditions at various magnetic field strengths. Unless noted in the figure legend, the presented data was collected at 600 MHz.